Original Research

17β-estradiol alters mRNA co-expression after murine muscle injury and mild hypobaria

Scott Emory Moore[1], Joachim G Voss[1] and Barbara St. Pierre Schneider[2]

[1]Frances Payne Bolton School of Nursing, Case Western Reserve University, Cleveland, OH 44106, USA; [2]School of Nursing, University of Nevada, Las Vegas, NV 89154, USA

Corresponding author: Scott Emory Moore. Email: sem167@case.edu

Impact statement

This study uses a murine model to address the clinical situation of transporting soldiers or civilians who have sustained skeletal muscle trauma by air. Our findings show that crush-injured muscle tissue of ovariectomized, 17β-estradiol-treated mice exposed to mild hypobaric hypoxia exhibited mRNA co-expression patterns among pathways associated with microtubule-dependent processes. Palmitoylation and other pathways necessary for movement of estrogen receptors to the cell membrane were also differentially enriched in the estrogen-treated mice. These first findings reframe the discussion regarding estrogen effects during muscle recovery from an inflammation-oriented inquiry to that of a structural, cytoskeletal inquiry and support additional research to understand the non-inflammation-related influences of estrogen during muscle recovery. Also, these results may suggest a role for estrogen or estrogen-like substances to treat muscle trauma.

Abstract

Here, we assessed the effects of 17β-estradiol exposure on mRNA co-expression patterns of muscle tissue during recovery in a closed muscle crush injury and hypobaria exposure murine model. Eighteen ovariectomized placebo-treated and 18 ovariectomized 17β-estradiol-treated female mice underwent closed muscle crush injury and hypobaric simulated flight. The mice recovered for 32, 96, or 192 h, and then were euthanized. Their harvested injured lateral gastrocnemius muscles underwent microarray analysis. We used weighted gene co-expression network analysis to construct a co-expression network for the control mice, and then applied the same network to the estrogen-treated mice. We compared the relationships between co-expression in gene modules over time between the two experimental groups. Enriched functional cluster analyses of significant co-expression network modules document a variety of different pathways of interest. Some of the functional cluster enrichments within several of the significantly correlated modules are related to the formation and function of microtubules. Our findings demonstrate that following a closed muscle crush injury in a murine model, the presence of 17β-estradiol alters mRNA co-expression patterns over time. It appears that estrogen promotes the expression of mRNA related to microtubule activity within the cytoskeleton of myofibers and in movement of organelles and receptors. Further study is needed, but the enrichment of these microtubule-related pathways may be integral in the muscle tissue regeneration process, and thus suggests that the presence of estrogen may promote muscle recovery through the work of the microtubules.

Keywords: Hypobaria, estrogen, closed muscle crush injury, microtubules

Experimental Biology and Medicine **2019; 244: 1454–1462. DOI: 10.1177/1535370219877360**

Introduction

Similar to other skeletal muscle injuries, a muscle crush injury can lead to high morbidity (e.g. shock and renal failure) and mortality.[1,2] In general, the early stage of pathophysiologic progression of muscle crush injury includes ischemia, necrosis, inflammation, reperfusion, and in the later stages, regeneration.[3–5] Estrogen is a key hormone that influences muscle tissue and is active in healthy and injured muscle, including both the early and later stages.

The benefit and roles of both endogenous and exogenous estrogens within muscle tissue have been reviewed extensively in the literature spanning human and animal models.[6,7] Exogenous estrogen therapies have been largely studied in non-injured tissues in order to describe how estrogen replacement affects skeletal muscle tissues, including muscle fiber size, gene expression, and tissue structure.[7–10] In a study of postmenopausal monozygotic twins, estradiol treatment via hormone replacement therapy was associated with cytoskeletal shape preservation

pathways, and the expression levels of those pathways explained 19% of the differences in relative thigh muscle proportion between the estrogen replacement exposed and nonhormone-replaced twins.[11] Cytoskeletal shape is influenced by the function of microtubule-related processes, and the connections between microtubules and muscle tissue responses to estrogen, including shape, function, organization, and differentiation, were also of interest to us in this study.[12–14]

Regarding the early stage of muscle recovery, estrogens are attenuators of inflammatory and immune responses.[15–20] However, the physiologic mechanisms of estrogen's influence on inflammation, immune response, and muscle healing vary across several rat and mouse models. For example, after downhill running, quadriceps femoris myofiber swelling occurred more slowly in female rats, and macrophage invasion and necrosis were less in this population.[21] In another downhill running experiment, estrogen treatment had an attenuating effect 24 h post-exercise on levels of infiltration of neutrophils in the white vastus muscle and macrophages in the injured soleus and white vastus muscles of ovariectomized rats.[22] In contrast, mouse muscle injury models have yielded differing results related to estrogens' effects on muscle inflammation. For example, in a study of lengthening contraction muscle injury in a mouse model, St. Pierre Schneider *et al*.[23] identified two sex-based inflammatory response differences: a later elevation of ER-BMDM1-positive leukocytes in female mice (seven days) than in male mice (five days), and fewer acid phosphatase-positive leukocytes in female mice injured muscle tissue one day after injury than in the males. However, in a different lengthening contraction injury mouse model study, St. Pierre Schneider *et al*.[24] did not find any leukocyte infiltration attenuation in ovariectomized mice receiving 17β-estradiol treatment. These differences in rat and mouse model findings are puzzling and leave several open questions as to why the mouse model results are different from the rat models. Some of these differences in the estrogens' effects on the early stages of muscle recovery may depend on the type of muscle injury, and understanding more about these differences remains an important scientific question.

In the later stages of recovery, injured muscle undergoes regeneration in which necrotic or damaged myofibers are replaced or repaired. Examining cardiotoxin-induced muscle tissue injury in ovariectomized mice, Kitajima and Ono[15] showed that estrogen increased the efficiency of satellite cells, noting estrogen-related differences in proportions of satellite cells in a state of myogenic differentiation vs. quiescence, but not an actual increase in the number of satellite cells per myofiber.[15] They also reported that when compared to ovariectomized mice, intact mice had a higher proportion of myonuclei per myofiber, which directly relates to satellite cells' role in producing myonuclei in muscle growth and regeneration. In contrast, Tiidus *et al*.[25] found that the number of satellite cells increased in male rats treated with estrogen 72 h after downhill running injury compared to the controls. Further, they reported that estrogens' stimulation of satellite cell activation and proliferation in post-exercise muscle appears to be carried out through estrogen receptor-alpha.[22,26] While these models are valuable for understanding the influences of estrogen on muscle growth, recovery, and inflammation, the differences related to model species, biological sex, mechanisms of injury, and other key study design components have not been fully described, and are worth further study.

Crush injuries of upper and lower extremities occur most frequently because of natural disasters, motor vehicle accidents, military conflicts, or through work-related injuries.[2,27] In many instances, long-distance aeromedical evacuation can be a critical factor in survival from these types of extremity trauma. However, during flight, the aircraft cabin is not pressurized to sea level (only to an altitude of 8000 ft), so the supply of environmental oxygen inside the cabin is lower than normal. Furthermore, not all injured people receive supplemental oxygen. Therefore, the likelihood of developing some degree of hypobaria-induced hypoxia is high, with one study noting 90% with at least one episode of noninvasive oxygen saturation less than 90%,[28,29] which may exacerbate tissue apoptosis and necrosis.[30,31] Goodman *et al*. simulated a 5-h hypobaric aeromedical evacuation flight of traumatic brain injured and sham-injured mice, and reported increased inflammatory markers (e.g. interleukin-6, macrophage inflammatory protein-1α) in cerebral tissue among the mice in the early (3 h post-injury) flight group, but not those in the delayed (24 h post-injury) flight group. Other results from prior studies examining the influence of aeromedical evacuation (through simulation) on muscle and limb injuries showed no association between increased edema[32] or extremity compartment syndrome[30]and evacuation. Kalns *et al*.[30] further reported that there was an increased quantity of some inflammatory cytokines (e.g. interleukin-1 beta, interleukin-6, tumor necrosis factor) in injured muscle tissue exposed to simulated flight.[30] Aeromedical evacuation can be a critical strategy to prevent the loss of limbs post crush injury, but it has been linked to inflammatory responses in injury of muscle and other tissues.

The aim of this study was to examine the effects of 17β-estradiol treatment on mRNA co-expression patterns in murine crush-injured skeletal muscle exposed to simulated aeromedical evacuation in a time-course experiment. The presence of estrogen in the ovariectomized mice resulted in different mRNA co-expression patterns over time when compared to placebo ovariectomized control mice. The pathways enriched within the treated mice co-expression patterns showed significant relationships with microtubules and microtubule-related processes. While enrichment of some immune and inflammatory-related pathways were also confirmed in our analyses, these microtubule-related findings are of interest because of their close relationships to estrogens' roles in the structure and function of muscle tissues identified in previously published studies discussed earlier. Therefore, these results support further exploration of the roles of estrogens and microtubules in the functions of muscle tissue and their roles at the cell- and tissue-level responses to injuries.

Materials and methods

Animals

Female C57BL/6NHsd ovariectomized (OVX) mice (six to eight weeks old, $n = 36$) were acquired from Harlan Laboratories (Indianapolis, IN, USA). Upon arrival to the pathogen-free facility, the mice were individually housed. A 12:12-hour light:dark cycle was implemented, with food and water as desired. All procedures were approved by the University of Nevada, Las Vegas Institutional Animal Care and Use Committee and the United States Air Force Animal Use Programs Office of Research Oversight and Compliance, and began after the mice had acclimated for at least five days in the facility.

Experimental procedures

Estrogen and placebo treatment. The ovariectomized mice were divided into control (OC, $n = 18$) and estradiol (OE, $n = 18$) groups. Those two groups were then divided into three euthanasia time point groups, targeting 32 h, 96 h (4 d), and 192 h (8 d) post-crush and representing different phases of muscle recovery. Before the mice underwent the crush injury procedure, pellets were implanted four to nine weeks after ovariectomy (day of placebo or estrogen treatment). The OC mice were administered a 60-day-release placebo pellet (Innovative Research of America, Sarasota, FL, USA; 0.18 mg total), and the OE mice received a 60-day-release 17-β estradiol pellet (Innovative Research of America, Sarasota, FL, USA; 0.18 mg total).

Closed muscle crush injury. On the eighth day of placebo or estrogen treatment, the crush injury procedure was performed. Mice were administered buprenorphine (Reckitt Benckiser Pharmaceuticals, Richmond, VA, USA), approximately 0.10 mg/kg subcutaneously, 1–5% inhaled isoflurane to effect and 100% oxygen. The crush injury was then applied to each mouse. The apparatus piston is in direct contact with the skin over the gastrocnemius and quadriceps muscles on the right side. Pressure was applied for 30 s at 45 psi for two to four applications. For a full description of the muscle crush model, see Dobek *et al*.[3] A second dose of buprenorphine was administered 10–12 h from the first dose.

Hypobaria exposure. Approximately 22–24 h following the crush injury procedure, the mice were exposed to hypobaria (565 ± 5 torr) for approximately 8–9 h, which was to a similar protocol as described in St. Pierre Schneider *et al*.[33]

Post-crush injury recovery and tissue harvesting

Each mouse was allowed to recover for approximately 32, 96, or 192 h post injury. Then, the mice were weighed and anesthetized with inhalant isoflurane (3–4%) and 100% oxygen. Next, blood was collected, and then the anesthetized mice underwent cervical dislocation. Uninjured or left and injured or right lateral gastrocnemius and quadriceps femoris muscles were harvested. The harvested samples were stored at –150°C after flash freezing in liquid nitrogen. Only the lateral gastrocnemius muscles underwent reverse transcriptase polymerase chain reaction. The uterine horns were also removed and weighed to calculate the relative uterine horn weight (RelUHW) as a proxy for estrogen bioactivity.[34]

RNA isolation and preparation

The RNA was extracted from the lateral gastrocnemius muscle using the RNeasy Fibrous Tissue Midi Kit (Qiagen, Valencia, CA, USA). Isolated RNA purity and concentration was determined using a Nanodrop ND-1000 (NanoDrop, Wilmington, DE, USA).

Microarray

Following RNA isolation and preparation, RNA samples were processed according to the Affymetrix GeneChip Whole Transcript Sense target labeling protocol (http://www.affymetrix.com/index.affx) for the Affymetrix Mouse Gene 1.0 ST array (Santa Clara, CA, USA). Arrays were scanned using an Affymetrix GeneChip® 3000 scanner. Image generation and feature extraction were performed using Affymetrix GeneChip Command Console software. The samples were processed at the microarray facilities of the University of Washington Department of Environmental & Occupational Health Sciences (DEOHS).

Statistical analyses

Microarray data preprocessing

Raw data from the Affymetrix GeneChip® scan were preprocessed for analyses using the 'frozen' robust multiarray analysis (fRMA) package for R.[35] This preprocessing algorithm performs background correction, normalization, and summarization of the raw microarray data. The preprocessing of the mRNA data was conducted by the DEOHS using fRMA version 1.14.0 for R (R: The R Project for Statistical Computing, version 3.0.2 for Windows, 09–25-2013) and Bioconductor (version 2.22.0).[36,37]

Weighted gene co-expression network analysis

We used a comparative systems analytical approach to identify mRNA co-expression networks among control and estradiol group samples. No samples were identified as outliers based on connectivity among the samples in a signed, correlation network of each observation, with a threshold of -2.5.[38] Then the preprocessed mRNA data were analyzed by treatment grouping (OCs, $n = 18$; OEs, $n = 18$) using the weighted gene co-expression network analysis (WGCNA) package for R.[39–41]

Both the statistical and biological underpinnings for WGCNA have been described.[38–41] In brief, our analysis was conducted based on standard WGCNA practices unless otherwise specified herein. We used the block-wise module function of the WGCNA package to construct the weighted gene co-expression networks. This function breaks the datasets into manageable blocks of 15,000, which allows for the inclusion of all 23,746 unique genes in the building of the modular network. We chose to use the

bicor (or biweight mid-correlation) and 'signed hybrid' options in WGCNA to calculate the pair-wise correlation adjacency matrices. To ensure all networks reach scale-free topology, we used a soft-thresholding level or power $\beta = 12$ for the treatment group-wise analyses.[40,41] Genes were then grouped together based on the similarity and dissimilarity of their connectivity patterns using a topological overlap measure (TOM) and a measure of dissimilarity of topological overlap (1-TOM) to compare and contrast the connectivity of genes within the network.[41] The genes were then hierarchically clustered based on the TOM and 1-TOM values, and the gene co-expression modules were identified using a dynamic tree-cutting algorithm. Once the initial block-wise analyses of all blocks of genes were completed, gene co-expression module assignments were reassessed across all blocks and genes were reassigned to modules where they have the highest connectivity. Module eigengenes (MEs) representing each module's first principal component were calculated, and highly correlated MEs ($r > 0.75$) were consolidated into one module where appropriate. Those genes not aligning with any of the modules were considered to be background genes and were assigned as members of the Grey module.[38,40]

The modules produced though WGCNA were composed of genes highly connected within the network constructed from the microarray data. The genes within the modules that were the most connected with other module member genes were considered to be hubs of the modules.[38,40]

We initially applied WGCNA to the OC data to identify the network and modular structure. In addition, the OC data capture mRNA expression in an ovarian hormone deficit state. Therefore, the OC data module assignments were used as the control network for all of our analyses, allowing for comparisons between the OC and OE data. We recognize that applying the OC module assignments to the OE data may have altered the structure of the network within the modules. However, those network structure differences observed (e.g. hub genes, top 500 genes) are essential to describing the influence that the presence of estrogen has on post-crush gene expression.

Treatment group network module-trait relationship analyses

The modules and their corresponding ME (module eigengene) values allowed us to examine correlations between modules and post-crush time (32 h, 96 h, or 192 h) and relative uterine horn weight (RelUHW). We also evaluated the modules for relationships with body weight at euthanasia as a control. We used biweight mid-correlation to evaluate associations between each module and the traits of interest.[38,40,41] Relationships between MEs and traits were considered significant at the $P < .05$ level. We made no corrections for multiple comparisons as the module-trait relationships are generative initial findings, leading to further inquiry both within and beyond the scope of this study.[42]

Identifying top genes in modules

We calculated a module membership value (kME) for each module identified through WGCNA for each gene in the dataset. The kME is equal to the correlation of each gene with each ME, and the strength of the correlation reflects how connected a gene is to the ME.[38,39] We constructed "top gene" lists for all non-Grey modules with a significant ($P < 0.05$) module-trait correlation with any of the three post-crush times or the RelUHW. For modules with less than 500 gene members, all genes were included, and for those modules with greater than 500 genes, we identified the 500 most "central" genes based on their kME for the module. Each dataset had its own list of top genes for each module, and because of the shared OC module assignments across both networks, common and unique genes were present in both sets of lists. Table 1 lists the top 10 genes from modules with significant relationships to post-crush time or RelUHW from both the OC and OE networks.

Top gene list functional annotation enrichment analyses

The top genes lists for each of the modules with significant relationships with post-crush time or RelUHW were analyzed for GO Term and KEGG Pathway enrichment using the Database for Annotation, Visualization, and Integrated Discovery (DAVID) Bioinformatics Resources version 6.8 website's Functional Annotation Clustering capabilities.[43] The DAVID Functional Annotation Clustering method allows for understanding relationships among genes in a list by evaluating gene lists for enrichment of individual GO Terms or KEGG Pathways and then evaluating the similarity among individually enriched annotations through a clustering approach. We utilized the default options for clustering and stringency for each list evaluated. The cluster enrichment *P*-value calculated by DAVID is expressed as the minus log transformed geometric mean of the enrichment *P*-values of all functional terms included in the cluster, setting a value ≥ 1.3 as the equivalent to a $P < 0.05$.[43]

Results

Ovariectomized control treatment group WGCNA network construction

The OC group mRNA expression data clustered into 18 non-Grey modules, each representing unique MEs, made up of 32 to 4727 genes each. The Grey module consisted of 2948 genes. There were no significant relationships between any MEs and mouse body weight at euthanasia or RelUHW in the OC group. The module that a gene is assigned to is consistent throughout these results. The clustered functional enrichments of the modules may differ to some extent between the OC and OE groups, as their mRNA co-expression patterns within the modules differ, and thus each gene's kME module membership value likely differs between the OC and OE co-expression networks. So while each OC module shares the same genes with the matching OE module, the co-expression patterns and relationships among the genes in the matching

Table 1. Top 10 hub genes of key modules in the ovariectomized control and ovariectomized estrogen-treated co-expression networks.

Brown	Green	Grey 60	Light Cyan	Midnight Blue	Pink	Red	Tan	Turquoise	Yellow
Top 10 hub genes in key modules of the OC co-expression network									
Uck2	*Angptl1*	***Gm3002***	***Hmgb1***	*Gnpnat1*	*D5Ertd577e*	*Myof*	***Rpl29***	***Acad11***	*Abca2*
Nup205	*Gpc4*	***Gm10406***	***Hmgb1-ps7***	*Sgpp1*	*E330014E10Rik*	*Serp1*	***Gm8580***	*Sucla2*	*Tmem248*
Slc3a2	*Sparcl1*	***Gm3696***	*Rps6*	*Pddc1*	*Clec3a*	*Plxnb2*	***Rpl28***	***Pdpr***	***9130011E15Rik***
Sh3bp2	***Plagl1***	***4930555G01Rik***	*Tcp1*	*Sptssa*	*C87414*	*Ms4a7*	*Pnlip*	*Fam120c*	*Smcr7l*
Pdpn	*H19*	***D830030K20Rik***	*Srsf5*	*Scarb1*	*9330020H09Rik*	*Yipf1*	*Gm10548*	*Tmem143*	*Slc25a38*
Pold3	*Pamr1*	***Gm5458***	*Tgds*	*Tmem67*	*Gm5622*	*Slc25a24*	*Phb2*	*Ppp6r2*	*Dnajb2*
Pcna	*Itm2a*	***Gm5796***	*Wtap*	*Pofut2*	*Magea3*	*Rps12*	*Gsto1*	*Fyco1*	*Herpud2*
Clptm1l	*Nrk*	***Gm2897***	*Snora44*	*Dynlt1a*	*Cecr6*	*Tmem173*	*Spry3*	*Man2a2*	*Vprbp*
Upp1	*Ssc5d*	*Pfn4*	*Chic2*	*Nme4*	*Muc19*	*Nucb2*	*Rag1*	*Socs7*	*Smg5*
Ubash3b	***Antxr1***	*Tex9*	*Klhl41*	*Mbip*	*Gpr142*	*Anxa1*	*Mrps2*	*Obscn*	*Cog1*
Top 10 hub genes in key modules of the OE co-expression network									
Tspan4	*Fam198b*	***Gm10406***	***Hmgb1***	*Dzip3*	*Spata20*	*Bcat1*	***Rpl29***	*Mpc2*	***9130011E15Rik***
Pcna	*Gbp6*	***Gm3002***	***Hmgb1-ps7***	*Armcx2*	*Ttc16*	*Actn1*	***Gm8580***	*Coq5*	*Hook1*
Gm6377	*Cdon*	***4930555G01Rik***	*Khdrbs1*	*Akt3*	*Taf7l*	*Kdelr2*	*Elovl4*	*Tmtc1*	*Ttll7*
Lpxn	*Hmcn1*	***Gm3696***	*Rps3a1*	*Fchsd2*	*Rbp2*	*Rnf26*	***Rpl28***	*Cacna2d1*	*Pdpk1*
Plek	*Gpc6*	***D830030K20Rik***	*Skap2*	*Slc2a10*	*Megf6*	*Iqgap2*	*Atp6v0c*	*Cep68*	*Msl3*
Anxa4	***Antxr1***	***Gm5458***	*Ubash3b*	*Slc36a4*	*Crygc*	*Entpd1*	*Gjb5*	*Klhl7*	*9630033F20Rik*
Capg	*Tmem131*	***Gm5796***	*Apbb1ip*	*Cntln*	*Ttll10*	*Stil*	*Alg3*	*Fbxo9*	*Ank3*
Tlr13	*Islr*	***Gm2897***	*Rpl15*	*Casp2*	*Chgb*	*Gnai2*	*Ftl1*	*Insr*	*Tom1l2*
Cndp2	*Ttc3*	*Mir376a*	*Rasgef1b*	*Eogt*	*Fbxo3*	*Ccnf*	*Hid1*	***Pdpr***	*Lmtk2*
Aprt	***Plagl1***	*Tspan12*	*Hnrnpd*	*Ska2*	*Nphs1*	*Cdc25b*	*Scamp4*	***Acad11***	*Rora*

Note: These are the 10 most centrally located genes from key modules identified during weighted correlational gene network analysis of mRNA expression. Key modules were identified as those with any significant correlation with post injury time or RelUHW.
OC: ovariectomized control; OE: ovariectomized estrogen-treated; RelUHW: relative uterine horn weight (calculated as uterine horn weight divided by necropsy weight); **Bold**: hub genes common between both networks.

modules differ, and thus the lists of top genes used for Functional Enrichment Analysis for the same color-named module from the two treatment groups, and by extension their enriched cluster results, may be different (see Table 1).

These MEs were related to post-crush time points in each group to identify significant correlations related to time and the presence of estrogen (see Figure 1).

Clustered functional enrichments of significant modules in OC mice. Among the OC mice, four MEs were significantly correlated with the 32-h post-crush time point, including OC Brown ($r = -0.67$, $P = 0.002$), OC Green ($r = 0.51$, $P = 0.03$), OC Red ($r = -0.58$, $P = 0.01$), and OC Turquoise ($r = 0.64$, $P = 0.005$); these four MEs have a combined total of 42 statistically significant functional enrichment clusters (see Table 2). At the 96-h post-crush time point, the only significant correlations were the OC Yellow module ($r = -0.53$, $P = 0.02$) and the OC Pink module ($r = -0.5$, $P = 0.04$). At the 192-h post-crush time point, there were a total of 27 significantly enriched functional clusters from the five MEs: OC Brown ($r = 0.7$, $P = 0.001$), OC Green ($r = -0.71$, $P = 0.001$), OC Yellow ($r = 0.63$, $P = 0.005$), OC Grey 60 ($r = -0.49$, $P = 0.04$), and OC Tan ($r = 0.5$, $P = 0.03$).

Clustered functional enrichments of significant modules in OE mice. In the OE group, there were six modules with significant module-trait relationships. Of those six modules, two had significant relationships with RelUHW, and there was no significant relationship between any module and mouse body weight. The OE mice mRNA expression patterns in five MEs were significantly correlated with the 32-h post-crush time, and combined, there were 49 statistically significant functional enrichment clusters identified among the top genes of the significant modules. The statistically significant correlations at the 32-h post-crush time included the following: OE Brown ($r = -0.62$, $P = 0.006$), OE Grey 60 ($r = 0.62$, $P = 0.006$), OE Light Cyan ($r = -0.48$, $P = 0.04$), OE Red ($r = -0.57$, $P = 0.01$), and OE Turquoise ($r = 0.57$, $P = 0.01$). There were four MEs significantly correlated with the 96-h post-crush time: OE Brown ($r = 0.51$, $P = 0.03$), OE Light Cyan ($r = 0.54$, $P = 0.02$), OE Midnight Blue ($r = 0.51$, $P = 0.03$), and OE Red ($r = 0.62$, $P = 0.006$). There were no significant associations with the 192-h post-crush time point in the OE network. See Table 2 for the OC and OE networks' thematic highlights of significantly functionally enriched clusters.

Discussion

Our findings demonstrate that following a closed muscle-crush injury in a murine model, the presence of 17β-estradiol alters mRNA co-expression patterns over time. Enriched functional cluster analyses of significant co-expression network modules document a variety of different pathways of interest. Many of the enriched clusters confirm functions expected in injury response (e.g. inflammatory and immune responses; OC/OE Brown, OC/OE Grey 60, OC Turquoise, and OE Light Cyan). We also report pathways in the functional cluster enrichments within several modules were related to microtubules (e.g. microtubules, microtubule-related movement; OC/OE Red). These microtubule-related enrichments differ

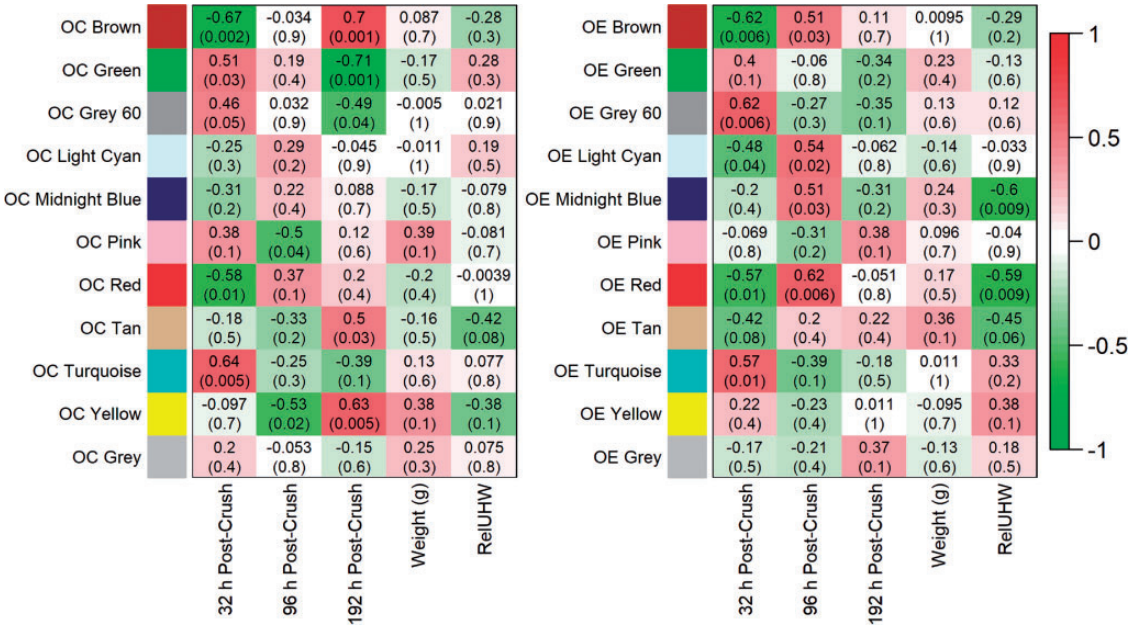

Figure 1. Co-expression module and mouse trait relationship heat maps in ovariectomized, control mice (OC) and ovariectomized, estrogen-treated mice (OE). Description: Heat maps show correlations between module eigengenes (rows) and traits (columns). Cells contain biweight mid-correlations and student asymptotic *P*-values; Red[positive]-Green[negative] cell color gradients represent correlation direction and strength (scale at right). Traits include post-crush times (32 h, 96 h, and 192 h), mouse weight (grams) at necropsy, and relative uterine horn weight (RelUHW, a proxy measure for estrogen, RelUHW=uterine horn weight (UHW)/necropsy weight). Note: Due to excess adipose tissue, UHW was not measurable in one 192-h OC mouse; instead, the 192-h OC group average UHW was used.

Table 2. Functionally enriched pathways by module and post-crush time.

Modules	Significant post-crush time correlations (*P*-value)			Functionally enriched pathway themes (total number significantly enriched clusters)
	32 h	96 h	192 h	
OC Brown	r = −0.67 (*P* = 0.002)		r = 0.7 (*P* = 0.001)	Smooth endoplasmic reticulum, protein folding, transport, stabilization; neutrophil, lymphocyte, monocyte chemotaxis (8)
OC Green	r = 0.21 (*P* = 0.03)		r = −0.71 (*P* = 0.001)	Proteostatic functions including proteolysis (6)
OC Grey 60			r = −0.49 (*P* = 0.04)	Immune cell chemotaxis, chemokine and cytokine signaling (5)
OC Pink		r = −0.5 (*P* = 0.04)		(0)
OC Red	r = −0.58 (*P* = 0.01)			Microtubules, microtubule-related movement, nucleosomes (13)
OC Tan			r = 0.5 (*P* = 0.03)	Glucose homeostasis, aerobic respiration (3)
OC Turquoise	r = 0.64 (*P* = 0.005)			Phagocytosis, natural killer cell mediated cytotoxicity, apoptotic signaling, chemotaxis (15)
OC Yellow		r = −0.53 (*P* = 0.02)	r = 0.63 (*P* = 0.005)	tRNA binding, collagen organization, proteasome function, translation initiation (4)
OE Brown	r = −0.6 (*P* = 0.006)	r = 0.51 (*P* = 0.03)		Endoplasmic reticulum function, stress responses; chemotaxis of macrophages, neutrophils, eosinophils, monocytes (9)
OE Grey 60	r = 0.62 (*P* = 0.006)			Chemotaxis of macrophages, neutrophils, eosinophils, monocytes; limb morphogenesis, mesenchymal cell proliferation regulation (6)
OE Light Cyan	r = −0.48 (*P* = 0.04)	r = 0.54 (*P* = 0.02)		Arp2/3 protein complex, Arp2/3 mediated actin nucleation; chemotaxis of macrophages, neutrophils, eosinophils, monocytes (16)
OE Midnight Blue[a]		r = 0.51 (*P* = 0.03)		Protein palmitoylation processes, cell projection organization, cilium morphogenesis (6)
OE Red[a]	r = −0.57 (*P* = 0.01)	r = 0.62 (*P* = 0.006)		Microtubules, microtubule-related movement, TCA Cycle, nucleosomes (9)
OE Turquoise	r = 0.57 (*P* = 0.01)			Glycogen metabolism, glucagon signaling processes, oxidative phosphorylation, nucleosomes (9)

OC: ovariectomized control; OE: ovariectomized estrogen-treated; RelUHW: relative uterine horn weight (calculated as uterine horn weight divided by necropsy weight).

[a]Significant correlation with RelUHW [OE Midnight Blue: r = −0.06, *P* = 0.009; OE Red: r = −0.059, *P* = 0.009.

between the OE and OC groups, and while both groups show suppression at the 32-h post-crush time, the mRNA from the 17β-estradiol-exposed mice had significant positive correlations at 96-h post-crush that were higher than the control mice. These findings bolster the hypothesis that estrogen supports microtubules' functions within crush-injured muscle tissue. Further, here we suggest that future studies should explore the roles of estrogens in microtubule functions—specifically in two key areas: (1) regulation of microtubules' function within the actin cytoskeleton of myofibers, and (2) microtubule-based movement of organelles and receptors (including estrogen receptors) inside the cell and to and from the cell membrane. The structure and function of microtubules are dynamic, and many of the same pathways and structural components are involved across the many roles of microtubules, and thus these two key areas may have some overlap with each other.

The functional enrichment analysis suggests a high level of activity in the co-expression of mRNA related to microtubules, both through the pathways directly related to the structure and functions of microtubules (e.g. OC/OE Red), and those associated microtubules' functions (e.g. actin cytoskeleton regulation pathway enrichment in OC/OE Brown and OE Grey 60). The actin cytoskeleton and the microtubule framework have both been identified as key components of skeletal muscle cell regeneration, maintenance, and repair processes.[44,45] Describing their functioning together and separately within injured skeletal muscle both with and without estrogen present is important in further explorations of estrogens' treatment potential. The link between microtubules and estrogen has been noted in postmenopausal women receiving hormone replacement,[11] but as of yet has not been described in muscle damage models. These relationships between enriched pathways support the importance of microtubules and actin cytoskeleton in the repair processes of skeletal muscle, thus improving estrogen's potential as a treatment to influence these processes is key to better understanding the differences in mRNA co-expression.

The function of the microtubules and other cell components in the preservation, manipulation, and alteration of the cell membrane and cytoskeleton is important for cell growth, motility, migration, and many other key functions.[46–48] Both actin fibers and microtubules are important for the movement of cells within muscle tissue, and many of these processes are associated with the Arp2/3 complex required for nuclear positioning in skeletal muscle regeneration (OC Turquoise, OE Brown, OE Light Cyan).[49–51] The enriched pathways identified in our findings reflect these linkages between the microtubules and the cytoskeletal shape, and further support the need to understand the influence of estrogen on the function and structure of microtubules in skeletal muscle tissues.

Another important role of microtubules in skeletal muscle tissue is the intracellular transport and movement of proteins, complexes, and organelles.[13] Nuclear movement and alignment can influence the differentiation and function of myocytes; the movement of nuclei along myotubes is a microtubule-dependent process.[13] The movement of these nuclei has been directly linked to progression of the muscle repair process.[52] Translocation of estrogen receptor monomers from the cytoplasm to the plasma membrane is also supported by microtubule-based movement. Estrogen receptors (ERs) are linked to multiple downstream effects, some of which involve promotion of protein biosynthesis and provide feedback to the cellular monitoring systems.[53,54] Their presence at the plasma membrane allows for initiation of processes within cells that may be important to the response to muscle cell injury. Two processes integral to the movement of ER monomers to the plasma membrane, S-palmitoylation of the ER monomer in the cytoplasm and movement of the ER monomer to the cell membrane via the microtubule network, are directly related to enriched pathways.[54,55] Once the ER monomer is palmitoylated, it interacts with cytoplasmic calveolin-1 protein, and then recruits heat shock protein-27. The palmitoylated ER monomer-calveolin-1 complex is then moved to the cell membrane via microtubules, and there it is available for interaction with extracellular estrogens to initiate one of several downstream processes.[54–58] Our findings suggest that the milieu of the injured skeletal muscle in the estrogen-treated mice may be supportive of these processes (OE Midnight Blue, protein palmitoylation processes). The presence of 17β-estradiol has been reported to influence different aspects of ER translocation processes (e.g. microtubule stability, ER expression).[56,59,60]

Conclusion

All of these findings taken together further supports our argument that estrogen-related benefits could be realized in a stronger microtubule and actin cytoskeleton matrix supporting the organization of organelles and receptors required for effective regenerative skeletal muscle repair processes. Understanding the differences in functional aspects of these mechanisms in the presence of 17β-estradiol is imperative for moving this line of inquiry forward. Future targeted protein studies with and without 17β-estradiol present will be key to understanding some of the functional influences implied by the mRNA expression data in this study. Further, in order to better understand the roles of the estrogens, future study designs should include both male and female mice; a mix of control, 17β-estradiol, and estrogen receptor antagonist treatments; examining time-series changes at shorter intervals; and consideration of pre-injury versus post-injury 17β-estradiol treatment models.

Authors' contributions: All authors participated in the design, interpretation, analysis of the data, and review of the manuscript; BSS and JGV conducted the experiments, SEM conducted statistical analyses, SEM, BSS, and JGV wrote and reviewed the manuscript.

DECLARATION OF CONFLICTING INTERESTS

The author(s) declared no potential conflicts of interest with respect to the research, authorship, and/or publication of this article.

FUNDING

This work was supported by a Department of Defense Air Force Grant (FA-7014–10-2–0001) awarded to Dr. Barbara St. Pierre Schneider. Dr. Moore's time during his postdoctoral fellowship training (2016–2018) was supported by the National Institutes of Health (T32 NR015433). Review of this material does not imply Department of the Air Force endorsement of factual accuracy or opinion. The content is solely the responsibility of the authors and does not necessarily represent the official views of the funders.

ORCID iD

Scott Emory Moore https://orcid.org/0000-0002-4294-1429

REFERENCES

1. Genthon A, Wilcox SR. Crush syndrome: a case report and review of the literature. *J Emerg Med* 2014;**46**:313–9
2. Jagodzinski NA, Weerasinghe C, Porter K. Crush injuries and crush syndrome – a review. Part 1: the systemic injury. *Trauma* 2010;**12**:69–88
3. Dobek GL, Fulkerson ND, Nicholas J, St. Pierre Schneider B. Mouse model of muscle crush injury of the legs. *Comp Med* 2013;**63**:227–32
4. Reis ND, Better OS. Mechanical muscle-crush injury and acute muscle-crush compartment syndrome. *J Bone Joint Surg Br* 2005;**87-B**:450–3
5. Speck K, St. Pierre Schneider B, Deashinta N. A rodent model to advance the field treatment of crush muscle injury during earthquakes and other natural disasters. *Biol Res Nurs* 2013;**15**:17–25
6. Enns DL, Tiidus PM. The influence of estrogen on skeletal muscle: sex matters. *Sports Med* 2010;**40**:41–58
7. Tiidus PM. Benefits of estrogen replacement for skeletal muscle mass and function in post-menopausal females: evidence from human and animal studies. *Eurasian J Med* 2011;**43**:109–14
8. Pöllänen E, Fey V, Törmäkangas T, Ronkainen PHA, Taaffe DR, Takala T, Koskinen S, Cheng S, Puolakka J, Kujala UM, Suominen H, Sipilä S, Kovanen V. Power training and postmenopausal hormone therapy affect transcriptional control of specific co-regulated gene clusters in skeletal muscle. *Age* 2010;**32**:347–63
9. Sipilä S, Taaffe DR, Cheng S, Puolakka J, Toivanan J, Suominen H. Effects of hormone replacement therapy and high-impact physical exercise on skeletal muscle in post-menopausal women: a randomized placebo-controlled study. *Clin Sci* 2001;**101**:147–57
10. Taaffe DR, Sipilä S, Cheng S, Puolakka J, Toivanan J, Suominen H. The effect of hormone replacement therapy and/or exercise on skeletal muscle attenuation in postmenopausal women: a yearlong intervention. *Clin Physiol Funct Imaging* 2005;**25**:297–304
11. Ronkainen PHA, Pöllänen E, Alén M, Pitkänen E, Puolakka J, Kujala UM, Kaprio J, Sipilä S, Kovanen V. Global gene expression profiles in skeletal muscle of monozygotic female twins discordant for hormone replacement therapy. *Aging Cell* 2010;**9**:1098–110
12. Cadot B, Gache V, Gomes ER. Moving and positioning the nucleus in skeletal muscle – one step at a time. *Nucleus* 2015;**6**:373–81
13. Gache V, Gomes ER, Cadot B, Blanchoin L. Microtubule motors involved in nuclear movement during skeletal muscle differentiation. *Mol Biol Cell* 2017;**28**:865–74
14. Robison P, Prosser BL. Microtubule mechanics in the working myocyte: microtubules in myocytes. *J Physiol* 2017;**595**:3931–7
15. Kitajima Y, Ono Y. Estrogens maintain skeletal muscle and satellite cell functions. *J Endocrinol* 2016;**229**:267–75
16. Routley CE, Ashcroft GS. Effect of estrogen and progesterone on macrophage activation during wound healing. *Wound Repair Regen* 2009;**17**:42–50
17. Stupka N, Tiidus PM. Effects of ovariectomy and estrogen on ischemia-reperfusion injury in hindlimbs of female rats. *J Appl Physiol* 2001;**91**:1828–35
18. Sugiura T, Ito N, Goto K, Naito H, Yoshioka T, Powers S. Estrogen administration attenuates Immobilization-Induced skeletal muscle atrophy in male rats. *J Physiol Sci* 2006;**56**:393–9
19. TiidusBombardier Oestrogen attenuates post-exercise myeloperoxidase activity in skeletal muscle of male rats. *Acta Physiol Scand* 1999;**166**:85–90
20. Voss JG, Shagal AG, Tsuji JM, MacDonald JW, Bammler TK, Farin FM, St. Pierre Schneider B. Time course of inflammatory gene expression following crush injury in murine skeletal muscle. *Nurs Res* 2017;**66**:63–74
21. Komulainen J, Koskinen SOA, Kalliokoski R, Takala TES, Vihko V. Gender differences in skeletal muscle fibre damage after eccentrically biased downhill running in rats. *Acta Physiol Scand* 1999;**165**:57–63
22. Enns DL, Iqbal S, Tiidus PM. Oestrogen receptors mediate oestrogen-induced increases in post-exercise rat skeletal muscle satellite cells. *Acta Physiol* 2008;**194**:81–93
23. St. Pierre Schneider B, Correia LA, Cannon JG. Sex differences in leukocyte invasion in injured murine skeletal muscle. *Res Nurs Health* 1999;**22**:243–50
24. St. Pierre Schneider B, Vigil SA, Moonie S. Body weight and leukocyte infiltration after an acute exercise-related muscle injury in ovariectomized mice treated with estrogen and progesterone. *Gen Comp Endocrinol* 2012;**176**:144–50
25. Tiidus PM, Deller M, Liu XL. Oestrogen influence on myogenic satellite cells following downhill running in male rats: a preliminary study. *Acta Physiol Scand* 2005;**184**:67–72
26. Thomas A, Bunyan K, Tiidus PM. Oestrogen receptor-alpha activation augments post-exercise myoblast proliferation. *Acta Physiol* 2010;**198**:81–9
27. Greaves I, Porter K, Smith JE. Consensus statement on the early management of crush injury and prevention of crush syndrome. *J R Army Med Corps* 2003;**149**:255–9
28. Goodman MD, Makley AT, Huber NL, Clarke CN, Friend LAW, Schuster RM, Bailey SR, Barnes SL, Dorlac WC, Johannigman JA, Lentsch AB, Pritts TA. Hypobaric hypoxia exacerbates the neuroinflammatory response to traumatic brain injury. *J Surg Res* 2011;**165**:30–7
29. Johannigman J, Gerlach T, Cox D, Juhasz J, Britton T, Elterman J, Rodriquez D, Jr, Blakeman T, Branson R. Hypoxemia during aeromedical evacuation of the walking wounded. *J Trauma Acute Care Surg* 2015;**79**:S216
30. Kalns J, Cox J, Baskin J, Santos A, Odland R, Fecura S. Extremity compartment syndrome in pigs during hypobaric simulation of aeromedical evacuation. *Aviat Space Environ Med* 2011;**82**:87–91
31. Skovira JW, Kabadi SV, Wu J, Zhao Z, DuBose J, Rosenthal R, Fiskum G, Faden AI. Simulated aeromedical evacuation exacerbates experimental brain injury. *J Neurotrauma* 2015;**33**:1292–302
32. Ritenour AE, Christy RJ, Roe JL, Dubick MA, Wade CE, Holcomb JB, Walters TJ. The effect of a hypobaric, hypoxic environment on acute skeletal muscle edema after ischemia-reperfusion injury in rats. *J Surg Res* 2010;**160**:253–9
33. St. Pierre Schneider B, Moonie S, Fulkerson ND, Nicholas J, Bammler T, Voss JG. Simulated flight, muscle genetics, and inflammatory indicators in mice. *Aviat Space Environ Med* 2013;**84**:840–4
34. Bond EF, Heitkemper MM, Perigo R. Gastric emptying and gastrointestinal transit in rats with varying ovarian hormone status. *Nurs Res* 1996;**45**:218–24
35. McCall MN, Bolstad BM, Irizarry RA. Frozen robust multiarray analysis (fRMA). *Biostatistics* 2010;**11**:242–53
36. R: The R Project for Statistical Computing, www.r-project.org/ (accessed 1 May 2018)
37. Huber W, Carey VJ, Gentleman R, Anders S, Carlson M, Carvalho BS, Bravo HC, Davis S, Gatto L, Girke T, Gottardo R, Hahne F, Hansen KD, Irizarry RA, Lawrence M, Love MI, Macdonald J, Obenchain V, Oleś AK, Pagès H, Reyes A, Shannon P, Smyth GK, Tenenbaum D, Waldron L, Morgan M. Orchestrating high-throughput genomic analysis with bioconductor. *Nat Methods* 2015;**12**:115–21
38. Horvath S. *Weighted network analysis: applications in genomics and systems biology*. New York: Springer, 2011.
39. Langfelder P, Horvath S. Eigengene networks for studying the relationships between co-expression modules. *BMC Syst Biol* 2007;**1**:54
40. Langfelder P, Horvath S. WGCNA: an R package for weighted correlation network analysis. *BMC Bioinformatics* 2008;**9**:559

41. Zhang B, Horvath S. A general framework for weighted gene co-expression network analysis. *Stat Appl Genet Mol Biol* 2005;**4**:Article 17
42. Rothman KJ. No adjustments are needed for multiple comparisons. *Epidemiology* 1990;**1**:43–6
43. Huang DW, Sherman BT, Lempicki RA. Systematic and integrative analysis of large gene lists using DAVID bioinformatics resources. *Nat Protoc* 2009;**4**:44–57
44. McDade JR, Archambeau A, Michele DE. Rapid actin-cytoskeleton-dependent recruitment of plasma membrane–derived dysferlin at wounds is critical for muscle membrane repair. *FASEB J* 2014;**28**:3660–70
45. McDade JR, Michele DE. Membrane damage-induced vesicle–vesicle fusion of dysferlin-containing vesicles in muscle cells requires microtubules and kinesin. *Hum Mol Genet* 2014;**23**:1677–86
46. Pizon V, Gerbal F, Diaz CC, Karsenti E. Microtubule-dependent transport and organization of sarcomeric myosin during skeletal muscle differentiation. *EMBO J* 2005;**24**:3781–92
47. Sébastien M, Giannesini B, Aubin P, Brocard J, Chivet M, Pietrangelo L, Boncompagni S, Bosc C, Brocard J, Rendu J, Gory-Fauré S, Andrieux A, Fourest-Lieuvin A, Fauré J, Marty I. Deletion of the microtubule-associated protein 6 (MAP6) results in skeletal muscle dysfunction. *Skelet Muscle* 2018;**8**:30
48. Vanegas C, Joca H, Vandermeulen J, Khairalla R, Lederer WJ, Stains J, Ward CW. Skeletal muscle contraction alters microtubule properties that impact function. *Biophys J* 2018;**114**:505a–6a
49. Goley ED, Rammohan A, Znameroski EA, Firat-Karalar EN, Sept D, Welch MD. An actin-filament-binding interface on the Arp2/3 complex is critical for nucleation and branch stability. *Proc Natl Acad Sci U S A* 2010;**107**:8159–64
50. Havelková L, Nanda G, Martinek J, Bellinvia E, Sikorová D, Šlajcherová K, Seifertová D, Fischer L, Fišerová J, Petrášek J, Schwarzerová K. Arp2/3 complex subunit ARPC2 binds to microtubules. *Plant Sci* 2015;**241**:96–108
51. Roman W, Martins JP, Carvalho FA, Voituriez R, Abella JVG, Santos NC, Cadot B, Way M, Gomes ER. Myofibril contraction and crosslinking drive nuclear movement to the periphery of skeletal muscle. *Nat Cell Biol* 2017;**19**:1189–201
52. Folker E, Baylies M. Nuclear positioning in muscle development and disease. *Front Physiol* 2013;**4**:363
53. Menazza S, Murphy E. The expanding complexity of estrogen receptor signaling in the cardiovascular system. *Circ Res* 2016;**118**:994–1007
54. Yaşar P, Ayaz G, User SD, Güpür G, Muyan M. Molecular mechanism of estrogen–estrogen receptor signaling. *Reprod Med Biol* 2017;**16**:4–20
55. Acconcia F, Ascenzi P, Fabozzi G, Visca P, Marino M. S-palmitoylation modulates human estrogen receptor-α functions. *Biochem Biophys Res Commun* 2004;**316**:878–83
56. Levin ER. Extranuclear steroid receptors are essential for steroid hormone actions. *Annu Rev Med* 2015;**66**:271–80
57. Levin ER. Extranuclear estrogen receptor's roles in physiology: lessons from mouse models. *Am J Physiol-Endocrinol Metab* 2014;**307**:E133–E140
58. Mundy DI, Machleidt T, Ying Y, Anderson RGW, Bloom GS. Dual control of caveolar membrane traffic by microtubules and the actin cytoskeleton. *J Cell Sci* 2002;**115**:4327–39
59. Goswami C, Kuhn J, Dina OA, Fernández-Ballester G, Levine JD, Ferrer-Montiel A, Hucho T. Estrogen destabilizes microtubules through an ion-conductivity-independent TRPV1 pathway. *J Neurochem* 2011;**117**:995–1008
60. Hatae J, Takami N, Lin H, Honda A, Inoue R. 17β-Estradiol-induced enhancement of estrogen receptor biosynthesis via MAPK pathway in mouse skeletal muscle myoblasts. *J Physiol Sci* 2009;**59**:181–90

(Received July 10, 2019, Accepted August 29, 2019)